Structural and magnetic transitions in $Gd_5Si_xGe_{4-x}$ $(0 \leq x \leq 0.9)$ from neutron powder diffraction

D. H. Ryan,[1] J. M. Cadogan,[2] L. M. D. Cranswick,[3,*] Karl A. Gschneidner, Jr.,[4,5] V. K. Pecharsky,[4,5] and Y. Mudryk[4]
[1]*Centre for the Physics of Materials and Physics Department, McGill University, Montréal, Quebec, Canada H3A 2T8*
[2]*Department of Physics and Astronomy, University of Manitoba, Winnipeg, Manitoba, Canada R3T 2N2*
[3]*Canadian Neutron Beam Centre, NRCC, Chalk River Laboratories, Chalk River, Ontario, Canada K0J 1J0*
[4]*Ames Laboratory of the U.S. Department of Energy, Iowa State University, Ames, Iowa 50011-3020, USA*
[5]*Department of Materials Science and Engineering, Iowa State University, Ames, Iowa 50011-2300, USA*
(Received 3 August 2010; revised manuscript received 9 November 2010; published 3 December 2010)

$Gd_5Si_xGe_{4-x}$ $(0 \leq x \leq 0.9)$ has been studied using neutron powder diffraction at a wavelength of 2.3724 Å. Antiferromagnetic ordering of the full 7 μ_B Gd moments in the *Pnm′a* magnetic space group is seen for Gd_5Ge_4, with the moments predominantly parallel to the *c* axis, with a significant *a*-axis component at the Gd $8d_2$ site. The remarkably strong (010) antiferromagnetic reflection has been used to map out the structural and magnetic phase diagram for this system and show that the O(II)→O(I) structural transformation never proceeds to completion in zero field. The absence of scattering that could be attributed to long-range FM order in the O(I) modification suggests that an externally applied field may be needed to stabilize the ferromagnetic state.

DOI: 10.1103/PhysRevB.82.224405 PACS number(s): 75.30.Sg, 61.05.F−, 75.25.−j

I. INTRODUCTION

The discovery of a giant magnetocaloric effect (GMCE) in $Gd_5Si_2Ge_2$ (Ref. 1) has led to an intensive effort to understand the magnetic and structural properties of the R_5X_4 compounds (where *R* is a rare earth, Y, La–Lu; and *X* is some combination of Si, Ge, and Sn) (Ref. 2) and a rich phenomenology of both coupled and distinct magnetic and structural transitions has emerged. Within the $Gd_5Si_xGe_{4-x}$ system, interest in freon-free refrigeration has centered on materials around $x=2$, where the coupled magnetostructural transition that leads to the GMCE occurs near ambient temperatures. However, the complex behavior at the Ge-rich end of the phase diagram $(0 \leq x \leq 1.2)$ has proven to be interesting in its own right.

Initial work on the room-temperature structure of $Gd_5Si_xGe_{4-x}$ showed that for $x \leq 0.95$, the system adopts the orthorhombic *Pnma* Sm_5Ge_4-type structure commonly denoted as O(II).[3] Beyond $x=0.95$, the system adopts the monoclinic (M) $Gd_5Si_2Ge_2$-type $P112_1/a$ structure. On cooling, the orthorhombic alloys order antiferromagnetically (AFM) (inferred primarily from bulk magnetic data) with a composition independent Néel temperature of about 130 K.[3,4] Further cooling leads to a marked change in behavior. There is a magnetostructural transition: the system becomes ferromagnetic (FM) and adopts the O(I) Gd_5Si_4 structure (derived from the same orthorhombic *Pnma* space group) which is also the room temperature form seen for $x>2$. Remarkably, this ferromagnetic O(I) form appears to be the ground state for *all* compositions in this system.[4] T_C was originally reported to fall linearly from about 115 K at $x=0.9$ to about 20 K by $x=0$.[3,4]

The O(II) phase boundary was later revised to lie at $x=1.2$ with the two magnetic transitions merging at $x \sim 1.0$ so that for $x>1.0$ only a single, first-order magnetostructural transition from the paramagnetic O(II) phase to the ferromagnetic O(I) phase is observed.[5] More importantly, the AFM→FM transition in Gd_5Ge_4 was found to be absent in zero applied field[6] and a more complex field/temperature phase diagram was developed.[7,8] In addition, the coupled O(II)→O(I)/AFM→FM transition was demonstrated to be irreversible below about 10 K, but reversible above about 20 K,[6] and an extensive phenomenology of glassy dynamics has been associated with the magnetostructural transition in Gd_5Ge_4.[9,10]

Given that the magnetostructural transition in Gd_5Ge_4 does not occur at all in zero field, it is not surprising that it was found to be incomplete in the Si-doped O(II) materials.[11,12] Initial work suggested that FM and AFM correlations persisted in structurally uniform samples at low temperatures,[11] however a more detailed structural and x-ray magnetic circular dichroism study showed that the samples were both magnetically and structurally inhomogeneous with AFM[O(II)]/FM[O(I)] regions coexisting below the onset of FM order.[12]

Normally, issues surrounding such complex magnetic and structural ordering would be resolved by using neutron diffraction. However, the extreme absorption cross section of natural gadolinium has discouraged such work and the limited information available on the magnetic structure of Gd_5Ge_4 has come from resonant x-ray scattering. X-ray resonant magnetic scattering (XRMS) measurements on a single crystal of Gd_5Ge_4 placed the Gd moments primarily along the *c* axis in the AFM ordered state, with FM *ac* slabs stacked AFM along the *b* axis.[13] A small *a* component could not be excluded, at all sites, while for the two Gd $8d$ sites, a small *b* component could be present, however, the Gd moments on all three crystallographic sites appeared to be equal, making a collinear *c*-axis AFM structure the most likely. Unfortunately, limited knowledge of absolute cross sections makes it impossible to determine the actual Gd moments by this method. This XRMS work was later extended to Si-doped compositions to follow the effects of temperature, field, and hydrostatic pressure on the magnetostructural inhomogeneity of these materials.[12]

We report here an extensive investigation of the magnetic ordering of $Gd_5Si_xGe_{4-x}$ ($x=0$, 0.1, 0.3, 0.5, 0.7, and 0.9)

using a recently developed large-area flat-plate technique which permits highly absorbing samples to be studied using neutron powder diffraction at the longer wavelengths needed for a detailed investigation of magnetic materials.[14] We are able to map out both the PARA[O(II)]/AFM[O(II)] and AFM[O(II)]/FM[O(I)] phase boundaries in zero applied field. We confirm the magnetic structure of the AFM[O(II)] ordered Gd_5Ge_4 and show that this structure is retained to $x=0.9$. The remarkably strong (010) magnetic reflection from the AFM[O(II)] ordered state allows us to follow the AFM[O(II)]→FM[O(I)] transformation in some detail and to detect the persistence of untransformed O(II) $Gd_5Si_xGe_{4-x}$ at 10 K all of the way to $x=0.9$ and residual fractions of less than 1%. Finally, we did not find the magnetic scattering expected to arise from ferromagnetic ordering of the O(I) form. As all existing reports of this FM ordering derive from bulk magnetization data where an external field is necessarily present while our neutron-diffraction measurements were made in zero field, this suggests that the stabilization of long-range FM order in the O(I) form of $Gd_5Si_xGe_{4-x}$ requires the presence of an external magnetic field.

II. EXPERIMENTAL METHODS

The six polycrystalline $Gd_5Si_xGe_{4-x}$ ($x=0$, 0.1, 0.3, 0.5, 0.7, and 0.9) samples were prepared at Ames Laboratory as described previously.[3,15] The samples were heat treated at 1300 °C for one hour to achieve a homogeneous atomic distribution and were then finely ground into micron-sized powders.

Approximately 150 mg of each powdered sample ($\sim 1/e$ thickness for absorption) was spread across a 2×8 cm^2 area on a 600-μm-thick single-crystal silicon wafer and immobilized using a 1% solution of GE-7031 varnish in toluene/methanol (1:1).[14] Neutron-diffraction experiments were carried out on the C2 multiwire powder diffractometer (DUALSPEC) at the NRU reactor, Canadian Neutron Beam Centre, Chalk River, Ontario. A relatively long neutron wavelength of 2.3724(1) Å was used so as to access the low-angle (010) magnetic reflection without interference from direct beam contamination. The plate was oriented with its surface normal parallel to the incident neutron beam in order to maximize the total flux onto the sample and the measurements were made in transmission mode. Temperatures down to 10 K were obtained using a closed-cycle refrigerator with the sample in a partial pressure of helium to ensure thermal uniformity. All measurements were made on cooling from 150 K so as to avoid artifacts from hysteresis associated with the first-order O(II)→O(I) structural transition. Where additional temperature points were needed, the sample was reset by cycling to 150 K for one hour before recooling. The majority of the patterns were measured for 5 h, however longer (20–30 h) reference patterns were taken at 150 K, 10 K, and at the maximum of the AFM[O(II)] signal for each sample.

Initial tracking of peak intensities was achieved by fitting Gaussian line shapes using a conventional nonlinear least-squares minimization routine. All full-pattern magnetic and structural refinements employed the GSAS/EXPGUI suite of programs.[16,17] The instrumental profile function was derived from silicon and Y_2O_3 standards run in the same geometry as the samples.[14] No absorption correction was applied, however, the data were truncated at $2\theta=60°$ to minimize the impact of angle-dependent absorption effects. The limited Q range considered ($Q<2.65$ $Å^{-1}$) and the low measurement temperatures used, greatly limit the effects of atomic vibrations on the observed diffraction patterns and so all thermal factors were set to zero. The strong absorption of thermal neutrons by natural gadolinium results from a low-lying nuclear resonance. This means that the scattering cross section is dominated by the imaginary term and is strongly dependent on energy. In order to determine the scattering length components appropriate to our neutron wavelength ($\lambda=2.3724$ Å and $E=14.54$ meV) we fitted data tabulated by Lynn and Seeger[18] with cubic polynomials, up to $E=40$ meV and interpolated to obtain estimates for the Real and Imaginary components of the scattering length of natural gadolinium for our neutron wavelength: 3.0 fm and −12.7 fm, respectively.

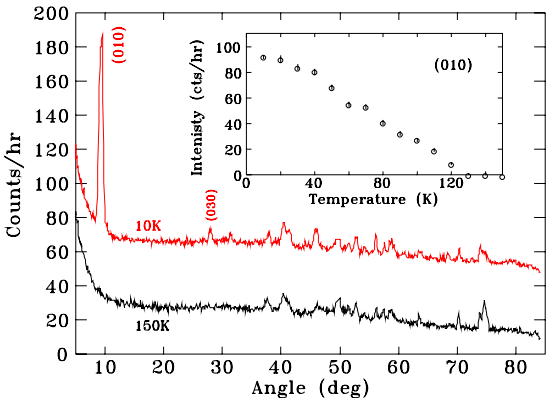

FIG. 1. (Color online) Comparison of neutron powder-diffraction patterns for Gd_5Ge_4 taken at 150 K (above T_N) and 10 K (well below T_N) showing the appearance of the striking (010) reflection near $2\theta=9°$ that results from the antiferromagnetic ordering of the gadolinium moments. The inset shows the temperature dependence of the (010) peak which gives an onset temperature of 129(1) K. Note that there is no reduction in the intensity of the (010) peak at low temperatures, confirming that the AFM[O(II)] form is not lost on cooling. The much weaker (030) reflection used in a recent XRMS study (Ref. 13) is also marked.

III. RESULTS AND DISCUSSION

A. Gd_5Ge_4

Cooling Gd_5Ge_4 through the expected T_N of about 130 K leads to the development of a remarkably strong AFM peak at $2\theta\sim 9°$ that can be indexed as the (010) reflection (Fig. 1). Comparison of the (010) line shape with that derived from standards shows that the peak is resolution limited and so reflects the presence of long-ranged AFM order as previously shown by XRMS.[13] The (010) peak is easily ten times stronger than any of the structural peaks observed above T_N in the 150 K pattern, and was observed in all of the samples studied here. It will be used below to track both the onset of the

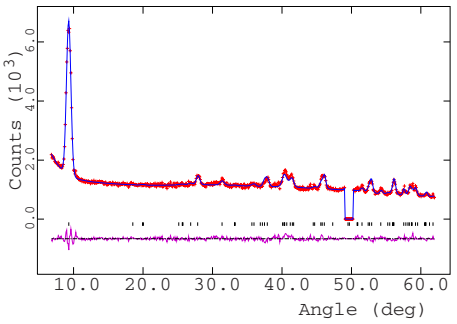

FIG. 2. (Color online) Full Rietveld fit to the diffraction pattern of Gd_5Ge_4 at 10 K. The data with fit are shown at the top and the residuals are given at the bottom. Bragg markers for the *Pnma* nuclear and *Pnm′a* magnetic scattering are shown between the data and residuals. The scattering is dominated by the (010) magnetic peak near 9°. Scattering from the sample mount near 50° was excluded from the fit.

AFM ordering and also to follow the transformation to the FM O(I) form in those compositions that undergo a structural change. The (030) reflection observed in an earlier XRMS study[13] is also present at $2\theta \sim 28°$ but it is more than 20 times weaker than the (010) reflection.

The determination of the magnetic structure of Gd_5Ge_4 is facilitated by consideration of the point symmetries of the three Gd sites in this orthorhombic structure. The Gd 4*c* site has the point group ·*m*·, i.e., a mirror plane whose normal is along the crystal *b* axis. Therefore, the allowed 4*c* magnetic modes are either: (a) ·*m*· with the Gd magnetic moment perpendicular to the mirror plane i.e., a *b*-axis moment. (b) ·*m′*· with the Gd magnetic moment lying in the *ac* mirror plane.

The point group of the Gd 8*d* sites is so there are no symmetry restrictions on either the magnitudes or directions of the magnetic moments at these sites. A complete description of the eight possible magnetic space groups, derived from *Pnma*, and their ordering modes for Gd_5Ge_4 has been given previously,[13] and so will not be repeated here.

A full Rietveld analysis of the Gd_5Ge_4 diffraction pattern taken at 10 K shown in Fig. 2 confirms that the Gd moments adopt the *Pnm′a* magnetic space group identified by Tan *et al.*[13] on the basis of XRMS data. Using standard notation, the allowed magnetic ordering modes at the Gd 4*c* and 8*d* sites, respectively, are G_xA_z and $G_x^-F_y^-A_z^-$ (which is written as $L_xP_yR_z$ in Ref. 13). The refined Gd magnetic-moment components are given in Table I.

One immediate advantage of neutron scattering over XRMS is that the cross sections are accurately known and corrections from multiple scattering are effectively absent so that absolute moments may be obtained rather than just ratios. Furthermore, by refining the entire pattern, more scattering contributions can be used and so more reliable conclusions about moment directions can be reached.

TABLE I. Fitted Gd moments for the three crystallographic sites in Gd_5Ge_4 at 10 K.

	Gd moments (μ_B)			
Gd site	*a*	*b*	*c*	Total
4*c*	0.9 ± 1.2	0	6.7 ± 0.3	6.8 ± 0.4
$8d_1$	0.3 ± 1.0	0	6.6 ± 0.3	6.6 ± 0.4
$8d_2$	2.3 ± 0.9	0	6.2 ± 0.2	6.6 ± 0.4

It is clear from the results given in Table I that the full 7 μ_B Gd moment is present at all three Gd sites in Gd_5Ge_4 at 10 K. The full-pattern refinement shows that the Gd moments at all three sites are directed primarily along the *c* axis, as noted previously by Tan *et al.*,[13] and that the *b* components of the Gd moments are all zero. This latter result is a requirement of the point symmetry of the 4*c* site which permits either *a* and *c* components, or only *b* components for the *Pnm′a* magnetic space group, but the ordering at the two 8*d* sites is not so constrained. Refinements carried out with the 8*d* moments completely unconstrained showed the *b*-axis components to be zero, within experimental error. Finally, we find clear evidence of an *a* component for Gd moments at least at the $8d_2$ site. The uncertainties for the 4*c* and $8d_1$ moment components preclude the assignment of anything other than pure *c*-axis order for these sites. While these ordering directions are consistent with calculations of magnetic anisotropy energies by Tan *et al.*[19] which showed that ordering along the *c* and *a* axes are clearly favored over *b*-axis order, the *a* component shown in Table I for the $8d_2$ site is much larger than the upper limit of ~0.05 μ_B derived from XRMS data.[13]

B. $Gd_5Si_xGe_{4-x}$

Replacing some of the germanium in Gd_5Ge_4 with silicon is expected to induce the coupled first-order O(II) $\rightarrow$ O(I)/AFM $\rightarrow$ FM transition at low temperatures.[5] The remarkable strength of the (010) reflection makes it an effective indicator of both the AFM ordering of the O(II) form and the loss of the O(II) phase as it transforms into the FM O(I) form. This expectation is clearly confirmed by the neutron-diffraction data for $Gd_5Si_{0.3}Ge_{3.7}$ shown in Fig. 3. The (010) peak near 9° develops steadily on cooling below 130 K and then almost completely disappears. The temperature dependence of the (010) peak intensity shown in Fig. 4 serves to emphasize the very different natures of the two transitions. The gradual increase in intensity on cooling through 130 K is characteristic of a second-order phase transition [the AFM ordering of the O(II) form] while the abrupt drop in intensity near 60 K (for $x=0.3$) reflects the first-order nature of the coupled magnetic and structural O(II) $\rightarrow$ O(I)/AFM $\rightarrow$ FM transition.

Increasing the silicon content from zero leads to a monotonic increase in the O(II) $\rightarrow$ O(I)/AFM $\rightarrow$ FM transition temperature while leaving the AFM transition in the O(II) form largely unaffected. However if we treat the (010) peak intensity at 10 K as an indicator of the presence of residual, untransformed O(II) phase, we can see from Fig. 4 that in many of the compositions the O(II) $\rightarrow$ O(I)/AFM $\rightarrow$ FM transition is far from complete, and once the material is a few tens of Kelvin below the transition temperature, no further evolution in phase composition is apparent. Given that the AFM transition temperature is largely unaffected by silicon

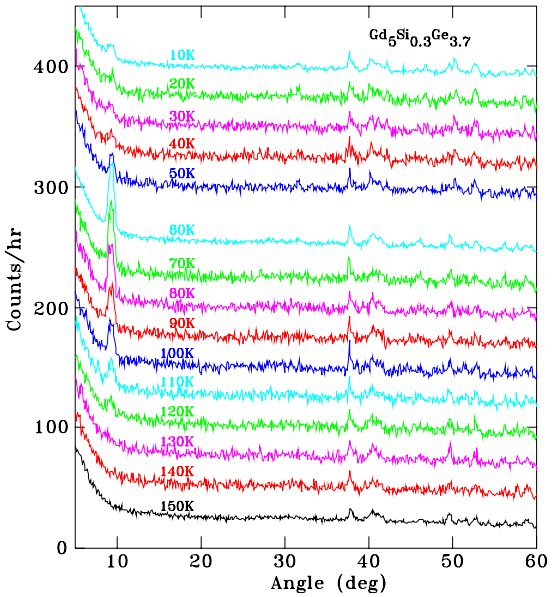

FIG. 3. (Color online) Neutron-diffraction patterns for $Gd_5Si_{0.3}Ge_{3.7}$ as a function of temperature showing the gradual growth of the (010) peak associated with the AFM ordering of the O(II) structure on cooling through 130 K followed by its abrupt and almost complete disappearance below 60 K as the O(II) form of $Gd_5Si_{0.3}Ge_{3.7}$ is converted to the FM O(i) form.

doping in the range studied here, and assuming that the magnetic structure and gadolinium moments in the AFM[O(II)] form are similarly stable, the intensity of the (010) peak can be used to obtain a quantitative estimate of the remaining O(II) phase in each sample at 10 K if we further assume that its intensity in Gd_5Ge_4 reflects its limiting value for no transformation. The results of this analysis are shown in Fig. 5

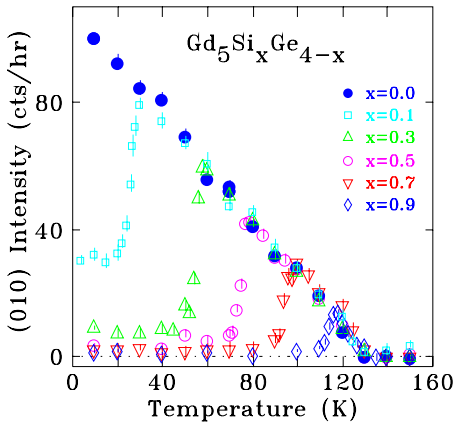

FIG. 4. (Color online) Temperature dependence of the (010) AFM diffraction peaks in $Gd_5Si_xGe_{1-x}$ showing the gradual growth through the second-order AFM transition near 130 K and its abrupt collapse at the first-order O(II)→O(I)/AFM→FM transition. It is clear that while T_N is essentially independent of x, the O(II)→O(I)/AFM→FM transition moves up toward T_N with increasing silicon content. The clear persistence of the (010) diffraction peak below the O(II)→O(I)/AFM→FM transition shows that the conversion to the O(I) does not run to completion, however it does become more complete with increasing x.

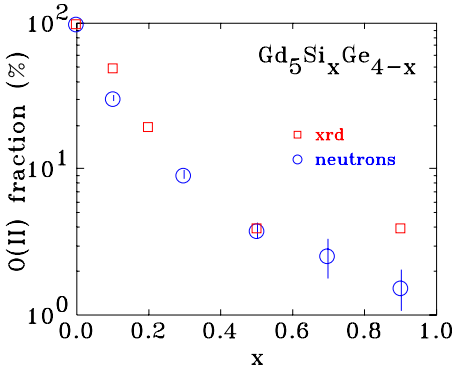

FIG. 5. (Color online) Normalized intensity of the (010) AFM diffraction peak measured at 10 K in $Gd_5Si_xGe_{4-x}$ as a function of composition showing the extent of the O(II)→O(I)/AFM→FM transformation at 10 K.

where they are compared with data taken from low-temperature x-ray diffraction measurements. It is clear that the agreement is extremely good and that the (010) reflection is a consistent and very sensitive indicator of the O(II) phase with an effective detection limit of less than 1%.

Taking the onset of intensity in the (010) peak as marking T_N and the midpoint in the drop in intensity of the same peak as an estimate of the O(II)→O(I)/AFM→FM phase boundary, we can construct the phase diagram shown in Fig. 6. While evidence from susceptibility and magnetization data indicate that the O(I) phase that forms on cooling the O(II) phase (for $0<x\leq 0.9$) is ferromagnetic, we were unable to detect any magnetic Bragg scattering from samples cooled into the O(I) region of the phase diagram. Simulations of likely magnetic structures all suggest that the expected signal should be easily visible in our diffraction patterns (at least comparable to some of the stronger nuclear peaks that we observed) so our failure to detect it strongly suggests that long-ranged ferromagnetic order is not present in the O(I) region of the phase diagram.

The remarkably strong (010) AFM peak seen in the O(II) form below T_N is an accident of the structure factor associated with this order. The next allowed peak, the (030), is 20

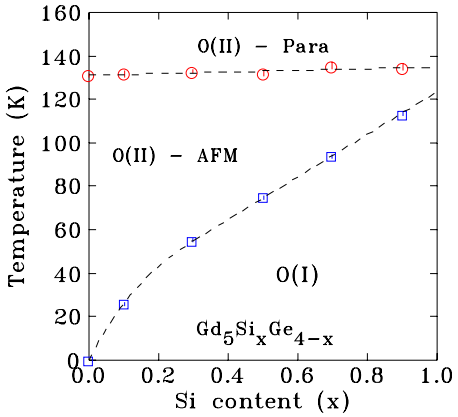

FIG. 6. (Color online) Structural and magnetic phase diagram for $Gd_5Si_xGe_{1-x}$ derived from our neutron powder-diffraction data. The O(II) form is clearly AFM below T_N, however no evidence for FM ordering of the O(I) form was detected (see text).

times weaker. The intensity of the (010) peak might lead one to expect similarly strong peaks to be associated with FM ordering in the O(I) form. This is however not the case. Our simulations show that the strongest FM peaks would be about ten times weaker than the (010): easily detected but not striking. If the FM correlation length remains finite, these peaks would be broadened and rendered invisible. Thus, if the ferromagnetic correlations in the O(I) form are only short ranged, we would not expect to see them.

It is possible that the disruption caused by the O(II) $\rightarrow$O(I) structural transition interferes with the spontaneous formation of a long-range ferromagnetic state and that true ferromagnetic order is only established in the presence of an external magnetic field. There is a clear precedent for such a situation in this system as Gd_5Ge_4 requires a field of order 2 T to drive the O(II) $\rightarrow$ O(I) structural transition below $\sim$30 K.[11,20,21] Furthermore, the dynamics of the field-driven transition are complex, dominated by strong irreversibilities.[10,22] The coexistence of the O(II) and O(I) forms below the structural transition was clearly seen here and has been noted before[11] while hydrostatic pressures of a few gigapascal have been shown to suppress the magnetic inhomogeneities that are observed in zero-field cooled samples.[12] It is apparent from the foregoing work that the mesoscale crystal and magnetic structures of these materials below the O(II) $\rightarrow$ O(I) transition line are complex, exhibiting significant time, field, and temperature dependencies.

All current evidence for the formation of a truly ferromagnetic state below the O(II) $\rightarrow$ O(I) line derives from measurements made in substantial external fields, and when taken with our failure to observe magnetic Bragg scattering below the O(II) $\rightarrow$ O(I) transition in zero field, we feel that it is inappropriate, at this time, to designate the O(I) form as spontaneously ferromagnetic. Further neutron powder-diffraction experiments directed at investigating this key issue are planned.

IV. CONCLUSIONS

Powder neutron-diffraction measurements of gadolinium-rich compounds at thermal wavelengths are not only possible but they yield key insights into the magnetic ordering of those compounds. The antiferromagnetic ordering of Gd_5Ge_4 has been confirmed using neutron powder diffraction at a wavelength of 2.3724 Å. The gadolinium moments are mostly parallel to the c axis with a small but significant a-axis component at the Gd $8d_2$ site. The remarkable intensity of the magnetic (010) reflection makes it an effective marker for the AFM[O(II)] phase and we have used it to confirm that Gd_5Ge_4 does not undergo the O(II) $\rightarrow$ O(I) structural transition that occurs in the silicon-doped materials. For $Gd_5Si_xGe_{1-x}$ ($x>0$) we have shown that the O(II) $\rightarrow$ O(I) transformation does not proceed to completion and even at $x=0.9$ about 1% of the sample remains in the AFM[O(II)] form at 10 K.

In constructing the structural/magnetic phase diagram we note that we did not find any evidence for long-range FM order at any temperature in any of the samples studied. It is possible that an externally applied field is essential to overcome the disorder caused by the O(II) $\rightarrow$ O(I) structural transformation and that long-range FM order does not occur spontaneously in the $Gd_5Si_xGe_{1-x}$ ($0<x\leq 0.9$) system.

This final and somewhat surprising observation serves to underline the value of using neutron diffraction to establish the true nature of the magnetic order in a system. We are currently designing experiments to follow up this work using an external magnetic field to stabilize the ferromagnetic state in the O(I) form of $Gd_5Si_xGe_{1-x}$.

Note added. After we completed this work we became aware of an independent study of $Gd_5Si_2Ge_2$ using hot ($\lambda \sim 0.5$ Å) neutrons where the authors report finding ferromagnetic order below the monoclinic (M) $\rightarrow$ O(I) structural transition in the much more Si-rich region of the $Gd_5Si_xGe_{1-x}$ phase diagram.[23]

ACKNOWLEDGMENTS

This work was supported by grants from the Natural Sciences and Engineering Research Council of Canada and Fonds Québécois de la Recherche sur la Nature et les Technologies. J.M.C. is grateful to the Canada Research Chairs program for its support. Work at Ames Laboratory is supported by the Office of Basic Energy Sciences, Materials Sciences Division of the U.S. Department of Energy under Contract No. DE-AC02-07CH11358 with Iowa State University.

*Deceased.

[1] V. K. Pecharsky and K. A. Gschneidner, Jr., Phys. Rev. Lett. **78**, 4494 (1997).

[2] K. A. Gschneidner, Jr., V. K. Pecharsky, A. O. Pecharsky, V. V. Ivtchenko, and E. M. Levin, J. Alloys Compd. **303-304**, 214 (2000).

[3] V. K. Pecharsky and K. A. Gschneidner, Jr., J. Alloys Compd. **260**, 98 (1997).

[4] L. Morellon, J. Blasco, P. A. Algarabel, and M. R. Ibarra, Phys. Rev. B **62**, 1022 (2000).

[5] A. O. Pecharsky, K. A. Gschneidner, Jr., V. K. Pecharsky, and C. E. Schindler, J. Alloys Compd. **338**, 126 (2002).

[6] E. M. Levin, K. A. Gschneidner, Jr., and V. K. Pecharsky, Phys. Rev. B **65**, 214427 (2002).

[7] E. M. Levin, V. K. Pecharsky, K. A. Gschneidner, Jr., and G. J. Miller, Phys. Rev. B **64**, 235103 (2001).

[8] C. Magen, L. Morellon, P. A. Algarabel, C. Marquina, and M. R. Ibarra, J. Phys.: Condens. Matter **15**, 2389 (2003).

[9] M. K. Chattopadhyay *et al.*, Phys. Rev. B **70**, 214421 (2004).

[10] S. B. Roy, M. K. Chattopadhyay, P. Chaddah, J. D. Moore, G. K. Perkins, L. F. Cohen, K. A. Gschneidner, Jr., and V. K. Pecharsky, Phys. Rev. B **74**, 012403 (2006).

[11] F. Casanova, S. de Brion, A. Labarta, and X. Batlle, J. Phys. D: Appl. Phys. **38**, 3343 (2005).

[12] Y. C. Tseng, D. Haskel, N. M. Souza-Neto, Y. Mudryk, V. K. Pecharsky, and K. A. Gschneidner, Jr., Phys. Rev. B **78**, 214433 (2008).
[13] L. Tan *et al.*, Phys. Rev. B **71**, 214408 (2005).
[14] D. H. Ryan and L. M. D. Cranswick, J. Appl. Crystallogr. **41**, 198 (2008).
[15] V. K. Pecharsky and K. A. Gschneidner, Jr., Appl. Phys. Lett. **70**, 3299 (1997).
[16] A. C. Larson and R. B. von Dreele, Los Alamos National Laboratory Report No. LAUR 86-748, 2000 (unpublished).
[17] B. H. Toby, J. Appl. Crystallogr. **34**, 210 (2001).
[18] J. E. Lynn and P. A. Seeger, At. Data Nucl. Data Tables **44**, 191 (1990).
[19] L. Tan *et al.*, Phys. Rev. B **77**, 064425 (2008).
[20] V. K. Pecharsky, A. P. Holm, K. A. Gschneidner, Jr., and R. Rink, Phys. Rev. Lett. **91**, 197204 (2003).
[21] H. Tang, V. K. Pecharsky, K. A. Gschneidner, Jr., and A. O. Pecharsky, Phys. Rev. B **69**, 064410 (2004).
[22] G. K. Perkins, J. D. Moore, M. K. Chattopadhyay, S. B. Roy, P. Chaddah, V. K. Pecharsky, K. A. Gschneidner, Jr., and L. F. Cohen, J. Phys.: Condens. Matter **19**, 176213 (2007).
[23] E. Palacios, J. A. Rodríguez-Velamazán, G. F. Wang, R. Burriel, G. Cuello, and J. Rodríguez-Carvajal, J. Phys.: Condens. Matter **22**, 446003 (2010).